5

Description of Adsorbed Phases on Carbon Surfaces: A Comparative Study of Several Graphene Models

José L. Vicente and Alberto G. Albesa
Instituto de Investigaciones Fisicoquímicas Teóricas
y Aplicadas INIFTA, Depart. de Química
Facultad de Ciencias Exactas, UNLP
CC 16, Suc. 4 (1900) La Plata
Argentina

1. Introduction

Since it was first identified (Scheele, 1777), gas adsorption process had been investigated for more than two hundred years. Among the large number of phenomena nowadays recognized involved in adsorption, the attention of the scientific community was focused on two main issues. First, from the applied point of view, characterization of solid surfaces through the observed behavior of the adsorbed phase was pursued. Second, and from the more basic science perspective, elucidation of the nature and magnitude of the interaction forces for different experimental conditions and systems.

Taking into account that the behavior of adsorbed molecules depends on the properties of both the solid surface and the adsorbate itself, and for somehow exploring basic aspect of the problem, we focused our attention only in a set of basic carbonaceous substrates and a small groups of simple adsorbates.

We have organized this review in several sections, starting in Section 2 with a brief discussion of some carbonaceous surfaces associated to graphitic structures when they are considered at different scales. This section also deals with different carbon materials and their properties as well as how description of several basic structural units and orientation degrees emerge (Bandosz et al., 2003). In Section 3.1 the adsorption of different gases such as nitrogen, carbon dioxide, argon and methane are described, with special emphasis in the last one due to its environmental relevance (Beaver & Sircar, 2010; Wagner, 1996; Wuebbles, 2000). Three approach to study gas adsorption on graphite surfaces that tackle the problem from different points of view where discussed (Albesa & Vicente, 2008): i) semi empirical quantum mechanical (SQM) model for gas – graphite interaction; ii) Grand Canonical Monte Carlo (GCMC) simulations (D. Do & H. Do, 2005; Sabzyan & Babajani, 2005); and Mean–Field Approximation (MFA) of the lattice model. To emulate by GCMC simulations the interaction gas – surface several models are compared (Albesa et al., 2008), and then a unified description is utilized for the adsorption mechanism that therefore was not only merely based on the three above three mentioned theoretical tools, but also on experimental data. The results reveal changes occurred the adsorbed species, and also can be used to

evaluate interaction energy between the gas and the graphite surface as the coverage increases; these allow elucidating somehow the role played by the substrate in adsorption process at different pressures and temperatures (Llanos et al., 2003; Steele, 1974). Section 3.2 is devoted to study the adsorption of simple gases using graphitic curved surfaces, for this end we used abs initio density functional theory (DFT) calculations for graphene sheets whose surfaces had different curvature, and discuss the relation between these model systems and experimental data for adsorption on single wall carbon nanotubes (Albesa et al., 2009; Albesa et al. 2010). In section 4, Gas Separation, we present simulated adsorption isotherms obtained for two characteristic carbonaceous structures, graphite and single wall carbon nanotubes.

2. Relation between different carbon and graphitic surfaces

The great interest in graphitic surfaces stems from their high surface activity, associated with strong adsorbate–surface forces and large surface area. From the commercial point of view, such structures are generally cheap to produce, and can be prepared with different special characteristics. As a result of the strong covalent sp^2 bonding in graphite, the distance C – C in graphite (*0.142 nm*) becomes shorter than the van der Waals radius of carbon (*0.335 nm*) giving a surface density of 38.2 atoms/nm^2.

The need to improve this activity, in order to have greater adsorption capacity and selectivity in mixture separation, has motivated the development of new carbon structures, related direct or indirectly to the graphitic ones. In few years the studies that began changing simple graphitic surfaces, rapidly grow beyond the broad word of fullerenes (Harris, 2003) and reach new and more exotic structures like nanotubes and nanohorns (Dresselhaus et al., 1996).

The two most common allotropes of carbon that occur naturally are graphite and diamond. Graphite is assembled from parallel sheets of hexagonal carbon atoms arrays, each atom being linked to three other sp^2 hybridized carbon atoms by sigma bonds or length *0.1415 nm*. The value of the in–plane lattice constant is *0.2456 nm*. The parallel sheets, or graphene layers, or basal planes, are held in place by the delocalized p electrons and are *0.3354 nm* apart. Diamond is assembled forming a tree – dimensional tetragonal network where each carbon atom is linked to four other sp^3 hybridized atoms.

The C_{an} fullerenes are shell–like molecules consisting of n three–coordinated carbon atoms arranged as 12 pentagons and ½ (n – 20) hexagons where n is even, and greater than 20 except 22. In spite of great a number of these molecules have been detected experimentally, only a few high–purity fullerenes are produced in macroscopic quantities. Fullerene molecules are essentially polyhedral rather than spherical and, increasing the number of carbon atoms, each fullerene can exist as one of several different isomers.

Just like in order to obtain a fullerene one has to lose the original sheet constituted by hexagonal carbon rings (incorporating pentagonal rings to the atoms arrange), the single walled nanotube (SWNT) is other kind of structure where this not happen and graphene configuration is preserved. In other words, the unit cell of a SWNT is constructed from a portion of graphene sheet defined by the chiral vector C_h and the translation vector $\boldsymbol{T}$. If $\boldsymbol{a}$ and b are the basis vectors, the chiral vector, $\boldsymbol{C}_h = n\boldsymbol{a} + m\boldsymbol{b}$, connects two equivalent sites on the graphene sheet at an angle defined by the so–called Hamada indices (n,m). The unit cell of a carbon nanotube is obtained by rolling up the graphene sheet (T, C_h) and joining the edges perpendicular to $\boldsymbol{C}_h$ to form a cylinder. There are three classes of nanotubes, i.e., zig –

zag, armchair and, chiral, corresponding to $n \neq m = 0$, $n = m \neq 0$ and, $n \neq m \neq 0$ respectively. From the Hamada indices one can define the diameter $d = C/\pi$ and the length $l = \sqrt{3}\ C/d_R$ of the nanotube unit cell, where $C = a\ (m^2 + mn + n^2)^{1/2}$, $a = 0.246\ nm$. , and d_R the greatest common divisor of $2m + n$ and $2n + m$. Multi wall nanotubes (MWNT) are constructed from a number of concentric SWNT. Carbon nanotubes are easier to manufacture than fullerenes and present higher stability; these properties together with their interesting physicochemical behavior, have prompted a great deal of interest reflected in the extensive experimental and theoretical studies published in the last years.

Like in the case of fullerenes, the graphenic membranes can take a conical shape only adopting arranges that are not purely formed by hexagonal carbon rings. The apex has to be defined by one or more ring atom removed in order to reach a conical hat that lead to the form of fivefold (or smaller) rings (Yudasaka et al., 2008). One class of such conical structures with a particularly sharp apical angle are the single–wall carbon nanohorns (SWNH). Conical graphenic structures with wider opening angles (corresponding to fewer pentagons at the apex) sometimes form multilayer structures). The diameter of an individual SWNH ranges from 2 to 4 nm, and the length is 40 to 50 nm. About 2000 of them assemble to form a spherical aggregate with a diameter of about 100 nm. Three types of spherical aggregates are known and, are called dahlia, bud and seed because of their appearances. The dahlia aggregate has long cone – shaped tips sticking through its surface, while the bud aggregate does not. The seed aggregates have lower graphitization that the dahlia and bud aggregates, and their tubules are corrugates (Azami et al., 2008).

In so far as increase the complexity of the carbonaceous structure the long range order of the graphene sheet is lost, because of the curvature, the presence of apexes, etc. Considering, according to the vast amount of experimental data, the hierarchical structure of the activated carbons (Bandosz et al., 2003), they would constitute perhaps a greater example of the previous mentioned loss. The first level of the hierarchy are the so-called basic structural units (BSU) that consist of a few roughly aligned polyaromatic–like molecules or "layers" that generally not preserve the graphite order between them, and due to the presence of functional groups, interlayer spacing are generally greater than that of graphite. The BSUs are assembled to form regions of local molecular orientation (the second level of the hierarchy) which are in turn assembled in space to yield the complex structure of activated carbons.

3. Adsorption on carbon surfaces

3.1 Simple gas adsorption on open graphite surfaces

The literature offers numerous experimental and theoretical studies of the gas adsorption on open graphite surfaces, considering the case of spherical molecules, e.g., rare gases (Cheng & Steele, 1990; Nicholson & Parsonage, 1982), simple molecules, e.g., nitrogen, oxygen, carbon dioxide and, methane (Bottani & Bakaev, 1994; Kowalczyk et al., 2005), and more complexes like ethylene or phenol (Bertoncini et al., 2000; Bottani, 1999). However, from a technological point of view, most of these studies restrict their descriptions to special conditions, i.e., low pressures or temperatures, soft surfaces, weak interactions, etc. In spite the powerful theoretical tools developed in the last decades, from semi empirical and DFT calculations to canonical (CMC) and grand canonical (GCMC) Monte Carlo simulations, nowadays two significant constrains limit computer performances to deal with the adsorption on graphite. One is the number of molecules considered in the calculations, and

this frontier moves as fast as new computer facilities are developed. The other problem comes from the approximations adopted in each model. The structure of different adsorbates on the basal plane of graphite has been extensively studied using Monte Carlo and molecular dynamics, however, the validity of these results depend on the interaction potentials adopted. The interaction potentials used in almost all computer simulations are composed of two parts: fluid–fluid and fluid–surface interactions. Some years ago the proposal (Steele, 1974) of an approximate interaction potential between a spherical molecule and a graphite surface (averaged over carbon atoms) reduced and became accessible the expensive computation time. On the other hand many systems and/or conditions require the knowledge of the real potential beyond how well the adsorbate–adsorbate interactions are described. As in example, the variation of the entropy of adsorption with the coverage in the basal plane of graphite determines the shape of the adsorption isotherm (variation of the chemical potential), because in the submonolayer region of this homogeneous surface the adsorption energy varies slightly due to the adsorbate–adsorbate interaction and the main contribution to the change on the chemical potential comes from the entropy of adsorption. Different corrections were proposed to improve the approximate gas-surface interaction potential, considering two dimensional Fourier series expansions (Kim & Steele, 1992) or simply introducing adjusting prefactors.[32] In spite it was argue, according to different reasons (Bottani & Bakaev, 1994; Kowalczyk et al., 2005), that neglecting the energetic inhomogeneity of the surface along the graphite plane is not expected to affect the results significantly. However, considering all kind of results that are possible to be obtained from homogeneous surface potentials, one can hardly agree with this affirmation, at least at low temperatures. It's because energetic homogeneity assumption means all sites on the surface are equivalent then, during the simulations, the probability that a molecule remains in one site or another is the same. On the contrary, considering energetic inhomogeneity, a molecule adsorbed on a site of the surface can reach other more favorable site later, during the simulation steps, in order to reach equilibrium that means inhomogeneity requires more trials to obtain each simulated point, even at low coverage. Of course, while the differences can be considered negligible at very low coverage, as the pressure increase they become significant, i.e. all sites are not equivalent on the surface and there will be fewer molecules adsorbed in the monolayer, and so on.

Among the simple gases that can adsorb on graphite, now we concentrate our study on the case of methane. Different reasons have leading the interest in the adsorption of methane on carbonaceous surfaces in general and, on graphite in particular. Practical reasons come from the fact that natural gas, which is composed mostly of methane, provides an alternative to traditional liquid petroleum fuels because their environmental advantages and natural abundance. From the theoretical point of view, next to the numerous and complete descriptions about rare gases adsorption process, the interaction between methane molecules and graphite surfaces remain with many unknown subjects to study.

According to the previous arguments, all description of the adsorption process, even on a simple graphite surface, requires a previous microscopic knowledge of the interactions between gas molecules and the substrate and between adsorbed molecules, as well as the different configurations of these molecules on the surface. But describing the interaction potential between methane molecules and graphene surface by using classical quantum mechanical methods, for real systems (i.e. many molecules involved), becomes a task beyond regular computational costs. On the other hand we are interested more than absolute values of the adsorption energies on each site of the surface, about the relative

differences between one site and another and, most of all how the presence of neighboring adsorbed molecules modified the adsorbed system geometrically and energetically. To tackle these problems we performed PM3 semi–empirical and density functional theory (DFT) calculations of increasing numbers of adsorbed methane molecules on a graphite surface. To mimic the graphene plane we have chosen a planar polyaromatic molecule which has chemical characteristic similar to graphite sheet in many aspects, as is shown in Fig. 1. The interaction energy, ΔE, of n $(n = 1,\ldots, 4)$ adsorbed methane molecules, has been calculated by employing PM3 semiempirical methods as:

$$\Delta E = E(G - n\,CH_4) - \left[E(G) + E_a(n\,CH_4) \right] \quad (1)$$

where $E(G–n\,CH_4)$, $E(G)$ and $E_a\,(n\,CH_4)$ are energies of the graphite–methane complex, the isolated graphite sheet and the methane molecules corresponding to the same configuration but without the graphite surface respectively (Albesa & Vicente, 2008). The results obtained at PM3 level were subjected to further geometry optimizations using DFT calculations (Parr & Yang, 1989; Wang & Perdew, 1991) keeping the graphene structure fixed. In order to consider the interaction energy when different numbers of methane molecules approach the surface, we begin optimizing the geometry of the first methane molecule from various relative orientations with respect to the reference plane of graphite.

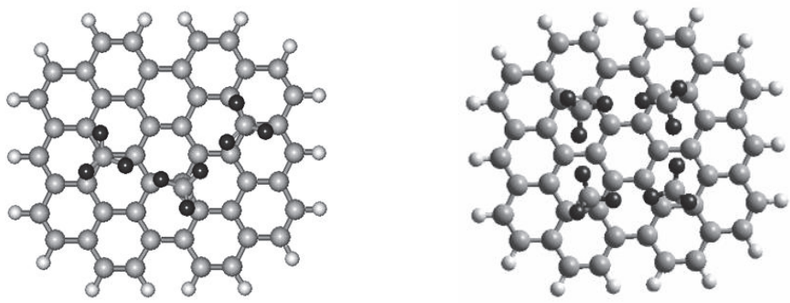

a) b)

Fig. 1. Optimized geometry of three and four methane molecules on a planar polyaromatic molecule that mimics a graphene surface (top view) (Adapted from Albesa & Vicente, 2008) Copyright 2008 Argentine Chemical Society

The interaction energy between methane and the graphite surface, at low coverage, is almost the same from one adsorption site to another. Although it seems to indicate that graphene structure does not play an important role in methane adsorption, one has to take into account that this result tell us only what happened at very low coverage, but says nothing about the consequences of neighboring adsorbed molecules, in other words, when the coverage increases how near the first adsorbed molecule next molecules can be placed?.

The interaction energy, corresponding to the most favorable configuration, between one, two, and three methane molecules adsorbed on a graphene surface, is almost the same ($\Delta E \cong -2.9$ *KJ/mol*). The distance of the adsorbed molecules to the surface diminishes from 4.2 Å for one molecule to 3.8 Å in the case of four from DFT results and 3.89 Å from PM3. Furthermore, the first three molecules form arrangements compatible with substrate hexagonal configuration of 4.5 Å sides, at almost the same distance of 3.95 Å from the

surface, this means that, with low coverage, the adsorbed phase follow graphene symmetry(see Fig 1a).

By increasing the coverage (i.e. four methane molecules), the structure is modified, the distance between methane molecules changes to 3.95 Å and between methane and graphene 3.80 Å, the interaction energy becomes ΔE (– 3.77 KJ/mol, and the hexagonal configuration move to a square one with the same average side of 4.5 Å (see Fig 1b). According to the previous quantum mechanical description of the interactions between gas molecules and the substrate and between adsorbed molecules, we conclude that, when equilibrium is reached, although at very low coverage a molecule has the same chance to adsorb on each site of the surface, letter as the coverage increase and some sites are already occupy, the probability that a molecule adsorbs in one site or another is not the same. In other words adsorption process can be approximated correctly considering energetic homogeneity of the surface at very low coverage, but when this condition is not fulfilled energetic inhomogeneity must be taken into account.

Computer Monte Carlo simulations (MCS) with the grand canonical ensemble (Albesa et al., 2008) is one of the more useful techniques that gives microscopic descriptions without expensive computational cost and allowing to over comes the quantum mechanical limitation of have to consider only a few adsorbed molecules. MCS offers not only the possibility of studying the adsorption phenomena at molecular scales but also making direct comparisons with experimental results. From the theoretical point of view MCS allow to compare how homogenous or non homogenous surface potential can be affect the results. We performed this comparison for the basal plane of graphite by taking the fluid–surface interaction (φ^{sf}) first, for the inhomogeneous case, as considering a two parameters 12–6 Lennard–Jones intermolecular potential between each atom of the adsorbate molecule (for methane we consider the spherical molecule approximation) as a site that interacts with each carbon atom of the solid, then the pair wise summation is carried over all atoms belonging to the solid that are located at a distance less than the cut off apart from the adsorbate mass center, and call this assumption atomistic model. Secondly, as an example of homogenous case we take the classical uniform Steele's 10 – 4 – 3 analytical potential (Steele, 1973)

$$\varphi^{sf}(z) = 3\varphi_w \left[\frac{1}{5}\left(\frac{\sigma^{sf}}{z}\right)^{10} - \frac{1}{2}\left(\frac{\sigma^{sf}}{z}\right)^{4} - \frac{\left(\sigma^{sf}\right)^{4}}{6\Delta(z+0.61\Delta)^{3}} \right] \tag{2}$$

where z is the distance between a fluid molecule and the substrate surface and Δ is the separation between lattice planes, the energy parameter φ_w si given by

$$\varphi_w = 4\,\pi\,\rho_s\,\varepsilon^{sf}\,(\sigma^{sf})^2 \tag{3}$$

being $\rho_s = 0.382\ Å^{-2}$ the carbon atoms density on the graphite slab surface, and the interaction parameters σ^{sf} and ε^{sf} are calculated using Lorentz – Berthelot combination rules. This approximation will be called analytical model. Then we compare the calculation by MCS with the grand canonical ensemble obtained from both models and with experimental results at different temperatures and pressures ranges.

At low pressures there is a good agreement between experimental and simulated isotherms for both models. In this pressure ranges, when the temperature changes, the curves exhibit different shapes. At temperatures lower than 113 K isotherms shows two clear horizontal

steps located at relative pressures of 13/40 and 29/40, respectively (see Fig. 2a), due to the completion of the first and second layers, that confirms an adsorption mechanism layer by layer (Hamilton & Goodstein, 1983). As the temperature increases, this kind of ordered adsorption is less significant, the steps are absent (see Fig. 2b) and all layers are available to be filled.

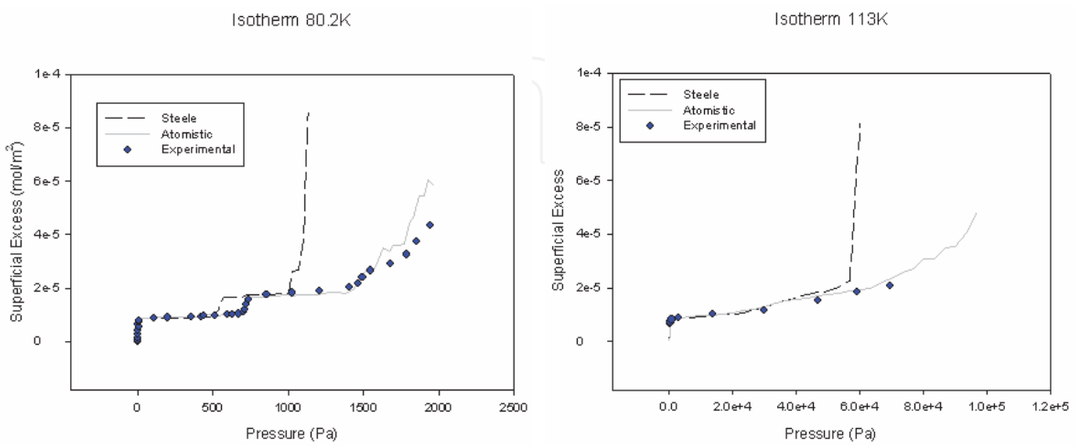

Fig. 2. Isotherms Circles are obtained from experimental results, and simulations are represented by dashed black lines for the analytic model and solid gray lines for the atomistic model. (a) 80.2K (b) 113K (Adapted from Albesa et al., 2008) Copyright 2008 American Chemical Society

In Figure 3 the density profile ρ*, as a function of the distance to the surface and the degree of coverage θ (adsorbed volume divided the monolayer volume), showed a series of peaks that allow to rationalized the mentioned layer–by–layer adsorption mechanism on one hand, and on the other hand exhibits differences between the results obtained from both models, because, the analytic model gives a denser (approximately 30%) phase that the atomistic model (see Figure 3). It is due to the fact that in the analytical approximation the surface is completely flat and smooth and methane molecules packing is more effective than in the atomistic model, which means that surface inhomogeneity becomes important. The difference becomes evident as pressure increase, because homogeneous approximation predicts condensation in advance after the third monolayer is formed (see Fig. 2a) instead of follow the real behavior, which is better fit by the atomistic model. In Fig. 3 one can also note that for the analytic model the layer equilibrium distances (mean density value) are closer to the surface than the corresponding to the atomistic model.

Among the thermodynamic aspects of gas adsorption on carbonaceous surfaces, enthalpy of adsorption study gives interesting and useful information about the process being accessible to experimental and theoretical explorations. From the experimental side both: direct methods like adsorption (Gravelle, 1978), flow (Groszek, 1998), differential scanning (Baudu et al., 1993), and immersion calorimetry (Zettlemoyer & Narayan, 1966); and indirect methods as inverse gas chromatography and adsorption isotherm have been widely employed last years. When the adsorbed phase is a rare gas, nitrogen, carbon dioxide or, methane on simple surfaces (graphene, single walled nanotubes, or nanocones), the use of adsorption isotherm measurements to determine the variation of adsorbed amount with temperature gives enough results to obtain accurate and reliable values of the heat of adsorption Q_{st} (Do, 1998).

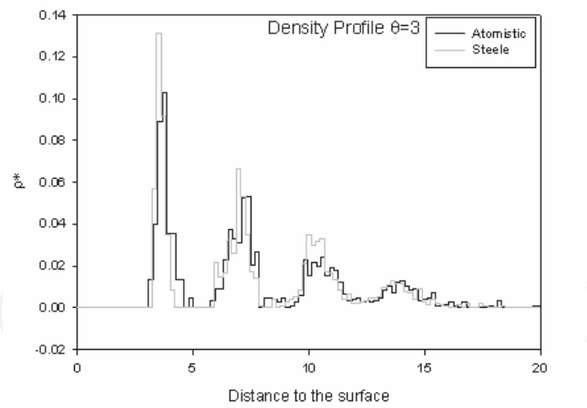

Fig. 3. Density profiles ρ* as a function of the distance to the surface in angstroms and the degree of coverage θ at 80.2 K when the isotherm is completed. Solid lines represent the results from the analytical model, and broken lines represent the atomistic model at θ = 3.0. (Adapted from Albesa et al., 2008) Copyright 2008 American Chemical Society

From two isotherms determined at similar but different temperatures, T_1 and T_2, a classical thermodynamic calculation gives:

$$Q_{st} = \frac{R\,T^2}{T_2 - T_1} ln\left(\frac{p_2}{p_1}\right) \tag{4}$$

where R is the gas constant, p_1 and p_2 are the equilibrium pressures at temperatures T_1 and T_2, respectively, when the adsorbed volume is constant and T is the corresponding mean temperature.

From the theoretical side the Computer Monte Carlo simulations (MCS) with the grand canonical ensemble not only gives the average number of molecules in the simulation box but also yields information about the isosteric heat, discriminating the two contributions, i.e. the solid–fluid interaction, and the fluid–fluid interaction. The isosteric heat of adsorption, $-\Delta H^0$, is defined as the difference between the molar enthalpy of adsorbate in the vapor phase, h_g, and the partial molar enthalpy of the adsorbed phase ($h_a = (\partial H_a / \partial N_a)_{p,T}$) (Pascual et al., 2003).

$$Q_{st} = \left\{ R\,T - \frac{\left[\langle E^g\,N\rangle - \langle E^g\rangle\langle N\rangle\right]}{\left[\langle N^2\rangle - \langle N\rangle^2\right]} \right\} - \frac{\left[\langle E^s\,N\rangle - \langle E^s\rangle\langle N\rangle\right]}{\left[\langle N^2\rangle - \langle N\rangle^2\right]} \tag{5}$$

The square–bracketed term in eq. 5 is the contribution of the fluid–fluid interaction to the isosteric heat of adsorption, whereas the last term is the contribution from the fluid–solid interaction. The isosteric heat of adsorption Q_{st} as a function of the coverage θ, for the system methane – graphite at lower temperatures was obtained from simulations by using equation 8 and is shown in Figure 4. We note, from both models, two clear peaks corresponding to the first and second layer completion. The Q_{st} values resulting from the atomistic and analytic models were 12.6 KJ/mol and 13.5 KJ/mol respectively, in good agreement with others values reported by Do and Do (D. Do & H. Do, 2005) (12.6 KJ/mol), and Piper and Morrison (Piper & Morrison, 1984) (13.4 KJ/mol). We can also see agreement between the analytic and atomistic models over the whole range of coverage except near the

firs monolayer completion, where the isosteric heat of adsorption given by the analytic model is 3 KJ/mol greater than the atomistic model value. In this region, there is a better agreement with the experimental results for the analytic model. The difference between both models is due to the fluid–solid contribution because the fluid–fluid contribution is the same in both models. To explain this one can take into account that the effective packing, obtained from the analytic model, gives a very well defined distance of the first layer to the surface (see. Fig. 3), as a consequence at very low coverage all molecules lay almost at the same distance from the surface, with a well defined fluid–solid interaction value. On the contrary the constrains of atomistic model determines greater dispersion of the first layer distance to the surface (see Fig. 3), and taking into account that there is a minimum distance that a molecule can approach to the surface, the layer becomes pushed away from the surface and the fluid–solid interaction, as well as the isosteric heat value, becomes lower.

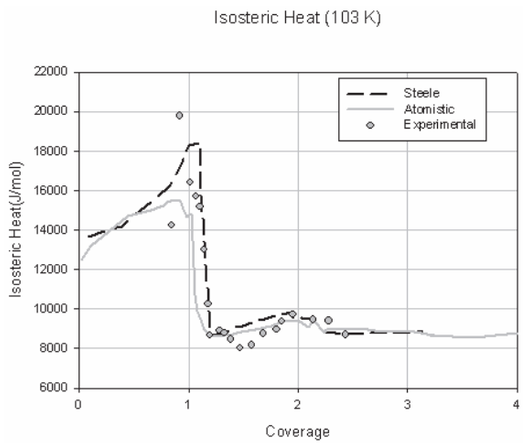

Fig. 4. Isosteric heat of adsorption as a function of the degree of coverage θ at 103 K. Circles are obtained from experimental results, and simulations are represented by dashed black lines for the analytical model and solid gray lines for the atomistic model. (Adapted from Albesa et al., 2008) Copyright 2008 American Chemical Society)

To describe the adsorbed system, aside quantum mechanical calculations, that gives answers at atomic level, where only a few molecules are analyzed; and Monte Carlo simulations (MCS) with the grand canonical ensemble, which explore at molecular level, where a more representative number of molecules is taken into account; the mean–field approximation (MFA) of the lattice model (De Oliveira & Griffiths, 1978) is other theoretical tool that that tell, at mesoscopic level, the behavior of adsorption isotherms of several layer of rare or simple gases adsorbed on graphite. According to the differences in the molecular density of the first layer obtain with the two mentioned models employed in MCS, the MFA could elucidate about this controversy. The mesoscopic level, where MFA operates, gives a global description of both the surface and the gas, but ignores what happens on the molecular level, and also assumes, a priori, a layer by layer adsorption process, being each layer constitutes by molecules adsorbed on a fixed lattice. These three mentioned techniques, in their respective ranges, give complementary information of the same phenomena.

Following the description of methane – graphite system, in the MFA one assumes, as in the lattice gas model (Burley, 1972), that the region above the substrate accessible to methane

molecules can be divided into cells whose centers forma a regular lattice. No more that one molecule is permitted in a cell, and each par of gas molecules in adjacent cells contributes an amount $-\epsilon$ to the potential energy. All molecules in the jth layer experience an additional potential energy $-v_j$ due to the substrate, with

$$v_j = \epsilon \left[\delta_{jl} D + \frac{(1-\delta_{jl})\, C}{j^3} \right] \tag{6}$$

The occupation number, n_{jk}, corresponding to the kth cell in the jth layer, take the values *0* or *1* if the cell is empty or occupied, respectively, then δ_{jk} is *1* when $k = j$ and *0* otherwise. C and D are proportional to the minimum energies for the interaction of a methane molecule with the semi – infinite continuous slab (9 – 3 potential) (Steele, 1974) and to the potential summation over different surfaces sites, respectively.

For each configuration $\{ n_{j\,k} \}$, the Gibbs – Boltzmann probability has to be proportional to $exp(-\beta H)$, where

$$H = -\epsilon \sum_{(j,k),(j',k')} n_{j\,k}\, n_{j'\,k'} - \sum_j (\mu + v_j) \sum_k n_{j\,k} \tag{7}$$

$\beta = (k_B T)^{-1}$, k_B the Boltzmann constant, T the absolute temperature, μ the gas chemical potential, apart from a temperature–dependent constant, and (j,k) denotes nearest neighbor pair of cells.

Calling ρ_j the average value of n_{jk} in the jth layer, the grand potential can be obtained, according to the MFA (Burley, 1972), by minimizing Ω, as a function of $\rho_1, \rho_2, \ldots$, where

$$\Omega L^2 = k_B T \sum \left\{ \rho_j \ln \rho_j + (1-\rho_j) \ln (1-\rho_j) \right\} - \sum \left(\mu + v_j \right) \rho_j - \epsilon \left[\frac{1}{2} a \sum \rho_j + b \sum \rho_j \rho_{j+1} \right] \tag{8}$$

L^2 is the number of cells in a single layer, and each cell has a number a of nearest neighbors in the same layer (related with the density of the layer), and b nearest neighbors just above it. At a minimum of Ω, the coupled set of equations

$$m_j = tanh \left\{ \frac{1}{2} \beta \left[\Delta\mu + v_j + \frac{1}{2} \epsilon \left(a\, m_j + b\, m_{j-1} + b\, m_{j+1} \right) \right] \right\} \tag{9}$$

is satisfied for $j = 1, 2, \ldots$. Here, $m_j = 2\,\rho_j - 1$ ($m_0 = -1$) and $\Delta\mu = \mu + \epsilon\,(a + 2\,b)/2$ is the chemical potential minus the resulting value for an adsorbed layer of infinite thickness.

To compute adsorption isotherms, eq. (9) is truncated at $j = 20$ ($m_{21} = m_\infty$), where m_∞ is the negative solution of

$$m_\infty = tanh \left\{ \frac{1}{2} \beta \left[\Delta\mu + \frac{1}{2} \epsilon \left(a + 2\,b \right) m_\infty \right] \right\} = 2\,\rho_\infty - 1 \tag{10}$$

The equation can be solved numerically for different values of a, b that are appropriate for each lattice configurations. For each value of β and $\Delta\mu$, the solutions that minimize eq. (7) are used.

Figures 5a and 5b show the results obtained taking $C = 12$ and $D = 20$, for the temperatures $T = 103\ K$ and $T = 171\ K$, respectively. It is noted that at low temperatures the isotherms

show greater dependence on the density of the condensed phase (associated with *a* and *b* values), and the better approach to the experimental results correspond to *a* = *6*, and *b* = *3*, corresponding to a triangular arrange compatible with results obtained with mechanical quantum calculation with three methane molecules. In addition the density associated with *a* = *6*, and *b* = *3*, fits experimental isotherms better than other values corresponding to higher densities (see Fig. 5a). When the temperature increases and approaches the critical value, this dependence disappears as is shown in Fig. 5b with different values of *a* and *b*.

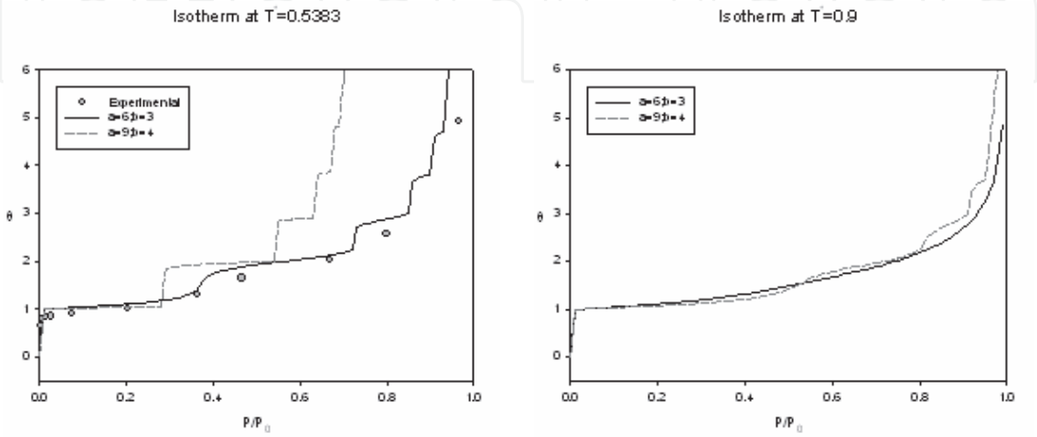

a) b)

Fig. 5. Experimental and lattice gas model isotherms at (a)103 K.(b) Experimental and lattice gas model isotherms at 171 K. (Adapted from Albesa et al., 2008) Copyright 2008 American Chemical Society

3.2 Simple gas adsorption on graphitic curved surfaces

Carbon nanotubes and in general microporous carbonaceous materials offer interesting properties from the technological point of view, as a mean to store hydrogen and methane (Bhatia & Myers, 2006), that are energy sources environmentally favorable, or as sieves to gas separations like oxygen and nitrogen (Arora & Sandler). Adsorptive properties of nanotubes and fullerenes differ from other graphitic carbons because of their carbon surface curvature (C–C–C bonding angles). Carbon atoms have to adopt quasi sp^2 hybridization due to their highly curved structure. The level of curvature of valence orbital depends on the material radius: great radius lead to hybridization near sp^2 pure, while small radius leads to sp^3 (Niyogi, 2002).

To describe phenomena that occur at molecular level one employs simulations, Monte Carlo grand canonical (Albesa et al., 2008) to study adsorption at equilibrium, or Molecular Dynamics (Cheng et al., 2005) when one is interested transport properties far from the equilibrium. However, the accuracy of these descriptions depend on the potential models adopted, choosing generally the 12–6 Lennard Jones potential, or the Crowell – Brown potential that don't take into account the surface curvature (Wang & Johnson, 1999). A correct potential has to identify the equilibrium position and to give a good approximation in its neighborhood, at least up to the curve inflexion point. To reach this it is necessary to have with a well description of the molecular bonds, because the approximations would neglect the effect of the hybridization differences of the carbon atomic orbitals, induced by

the curvature of the surface. To solve this problem force fields were derived (Kostov et al., 2002) where the curvature effect was taking into account, however, the parameters calculated for these fields overestimate the interaction of the nanotubes of smaller radius, because they are considered as a model molecule with free radicals.

In order to describe the potential energy that suffer a molecule near the surface of different nanotubes, theoretical calculations at DFT level were performed (Albesa et al., 2009) for hydrogen, nitrogen and methane, were the surface was mimicked by deforming a coronene molecule (see Fig 6). The nanotube diameters d can be described by the Hammada's indices (m,n), as $d = a/\pi\,(m^2 + mn + n^2)^{1/2}$ and, $a = 0.246\ nm$, employing "armchair" type ($n = m$), taking into account the independence of quirality for simple gases adsorption (Vilaplana, 2005).

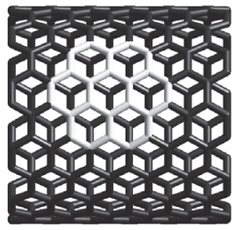

Fig. 6. Cluster carbon atoms employed in the calculations

The exploration involves diameters according to experimental values, that means, $d = 0.407$, 0.949, and $2.034\ nm$, corresponding in the Hammada's notation to $(3,3)$, $(7,7)$, and $(15,15)$ respectively. In spite of that results obtained from DFT (see Fig. 7), as almost all Generalized Gradient Approximation calculations, give energy values lesser that those obtained experimentally, i.e., $3.3\ KJ/mol$ for hydrogen (Okamoto & Miyamoto, 2001), and $10.5\ KJ/mol$ for methane (Talapatra & Migone, 2002), it is interesting to explore the relative values and their deviation when nanotubes diameter change. The interest on DFT results is because, beyond this approach gives lesser energy values than those experimentally obtained and a bad description very far from the surface, it allow to describe very well the relative energy potential behavior near the equilibrium point. As is shown in Figure 7a, the interaction energy of hydrogen as a function of the distance to the surface, resulting from DFT calculation, determines very low values on the nanotube external face, which tell as that storage this gas on closed nanotubes is rather difficult. We can also see that the values corresponding to the two smaller nanotubes are almost equal. In case of methane, showed in Figure 7b, one can see that the nanotube of the intermediate diameter has a fewer attractive potential with regard to the other two kind of nanotubes. If the curves are fitted with the classical 12–6 Lennard–Jones potential, the values obtained for the position of the potential minimum (σ) is almost the same for different nanotubes, around $0.37\ nm$, for hydrogen; and $0.402\ nm$, for methane, being $0.32\ nm$, and $0.36\ nm$ the values corresponding to the adsorption on graphite; and the deep potential well (ε) is, as the nanotube diameter increases, 7.4, 12.6, and $9.36\ K^{-1}$, for hydrogen; and 14.7, 12.6, and $14.9\ K^{-1}$, for methane. From these results one can conclude that the potential energy obtained doesn't show an important dependence on the curvature of the nanotubes, at least in the explored range.

The experimental isotherms for the adsorption of methane, measured at 77.3 K, unlike the case of the adsorption on graphite that has only one step in the monolayer regime (0.2 kPa), have one sub step below this pressure and other one above it (Albesa et al., 2010). As in the case of graphite when the temperature increases, this stepwise adsorption behavior is less pronounced, and above 103 K the substeps disappear.

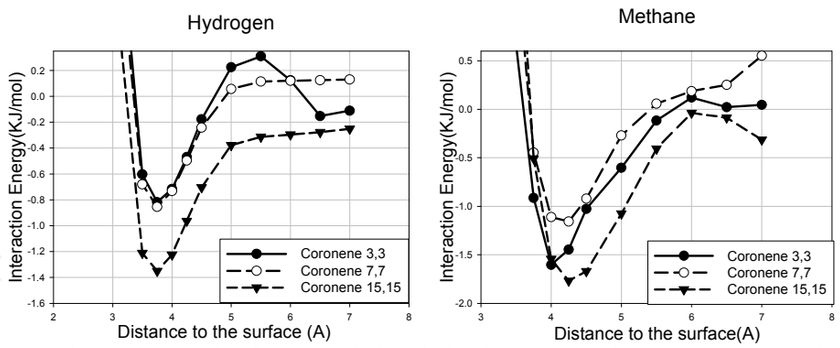

Fig. 7. Energy potential curve for (a) hydrogen molecule (b) methane molecule

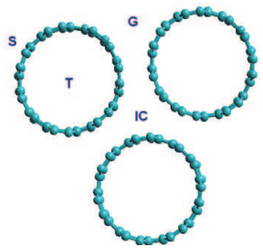

Fig. 8. Smaller simulation cluster, showing adsorption sites: the grooves (G) between two tubes; on nanotube surface (S); in interstitial channels (IC); and in the interior of a nanotube (T), for open tubes. (Adapted from Albesa et al., 2010) Copyright 2010 American Chemical Society

To explain this behavior, beyond the theoretical interest to explore the adsorption of simple molecules on the curved surface, that mimic the external environment of a nanotube, these kind of carbonaceous structures don't appear alone but forming different bundles of numerous tubes. These kind of arrange generate new potential adsorption sites, besides the mentioned sites on curved graphene, corresponding to sites on the external phase of the bundle external tubes. For single walled nanotubes (SWNT) four different adsorption sites has been identified (see Fig. 8), i.e. the previous mentioned convex external walls or outer surface sites (S), the interstitial channels (ICs), the grooves between two adjacent outer nanotubes of the bundle (G), and, in case of SWNTs open at the ends, the inner sites (T).
To describe the adsorption process, in closed SWNT, it has been proposed (Bienfait et al., 2004; Kuznetsova et al., 2000) that it starts as linear chains at the strongest binding energy sites: grooves on the outside surface of the bundles and some larger, accessible, defect – induced interstitial channels. After these sites are filled, adsorption proceeds on the external surface of the bundles. The 2D adsorbate structure on the external bundle surface initially builds up adjacent to the occupied grooves until the entire external surface is covered by a single monolayer. The binding energies for this latter stage of adsorption are comparable but somewhat smaller than for adsorption on the basal plane of graphite, whereas the binding energy on the preferential adsorption sites (G, IC) populated during the initial stage of adsorption is considerably larger that tat on the planar graphite. In order to elucidate between the more attractive sites like groove (G) and interstitial channels (ICs), which one begins to fill up first, it has been performed Ab Initio and Molecular Mechanical Calculations, for the case of methane. In order to mimic different sites (S, IC, G, and T) of

the substrate, a triangular array consisting of three identical tubes was used, this is the minimum bundle configuration that exhibits the four (S, IC, G) characteristic sites (see Fig. 8). The distance between the tubes or van der Waals gap always is taken equal to *0.34 nm*. Three different nanotube diameters were explored, i.e. *0.949*, *1.628*, and *2.034 nm*, or Hamada indices *(7,7)*, *(12,12)*, and *(15,15)* respectively. Although the last diameter (*2.034 nm*) is not realistic, it's enough large that the IC sites are able to accommodate a molecule and can mimic a general intertube channel that can appear in general tube bundles. In other words, the two first diameters were employed to analyze G, S and T (in case of open nanotubes) sites, and the last one to IC sites. As the molecular dynamics simulations, using MM+ force field, as the calculation employing ab initio density functional theory (DFT) (Albesa et al., 2010), tell that IC sites begin to fill before the G sites.

A complementary picture at molecular level, can be performed by Monte Carlo simulations (MCS) with the grand canonical ensemble, in order to take into account the behavior of a representative number of molecules in the adsorbed phase. Results showed in Figure 9, for tubes with a diameter of 2.034 nm, confirm the sequence of filling of different sites in the bundles (is spite of not being realistic, this diameter allows adsorption in IC sites, and the other sites follow the same steps, independent of the kind of nanotubes employed).

The isotherms of nanotubes of 1.628 nm of diameter at different temperatures (83, 93, and 113 K) are compared between closed and opened end in Figures 10 and 11. Unlike the closed end (Fig. 10), the opened end tube (Fig. 11) shows a knee when a monolayer starts forming on the inside surface of the nanotubes, and also when this interior layer is completed (Tasca et al., 2002), and a new high energy site appears in the axial phase (see Fig. 12). It can also mentioned the isotherms corresponding to smaller tubes (0.949 nm of diameter) exhibits only the first knee because there is no possibility of an inner axial phase.

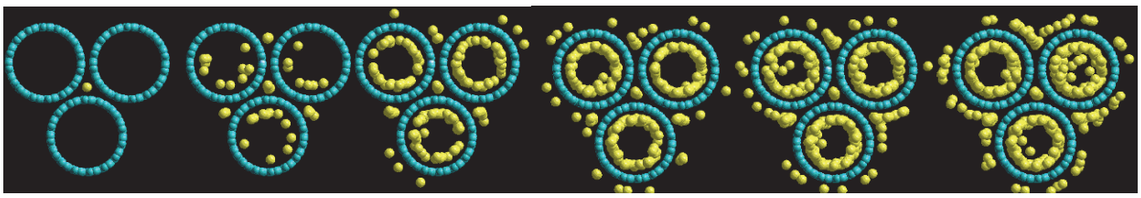

Fig. 9. Upper view of filling evolution corresponding to isotherm at 113 K and pressures of 0.0113, 5.09, 22.6, 50.9, 226, and 409 Pa for opened end tubes of 2.034 nm, (15,15) SWNT. (Adapted from Albesa et al., 2010) Copyright 2010 American Chemical Society

This dependence, of the adsorption process, on the nanotube diameter, suggests that it would be useful to classify the bundles according to the diameter of the tubes involved, analogous to the method used for porous substrates classification employing porous sizes.

Comparing simulated isotherms with the adsorption on graphite we note that the monolayer on graphite is completed at a pressure below that corresponding to the nanotubes, and that the isosteric heat of adsorption is greater for graphite. This is due to the greater gas – solid interaction for the graphite case, because the nanotubes are single – walled, while graphite is formed by several graphene layers. The gas – gas interaction on the nanotubes is weaker than on graphite, because the curvature of the nanotubes reduces the number of neighboring adsorbate molecules in this case, relative to those present in the graphite case.

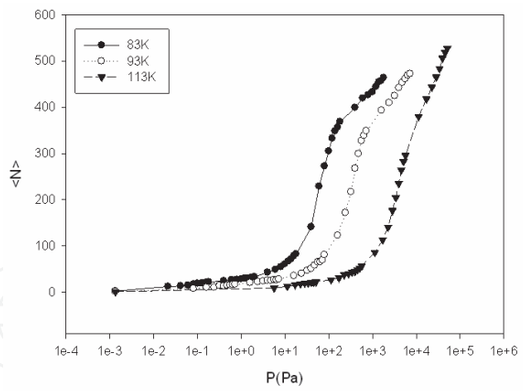

Fig. 10. Simulated isotherm at 83, 93, and 113 K for closed end tubes of diameter 9.52nm (7,7) SWNT. (Adapted from Albesa et al., 2010) Copyright 2010 American Chemical Society

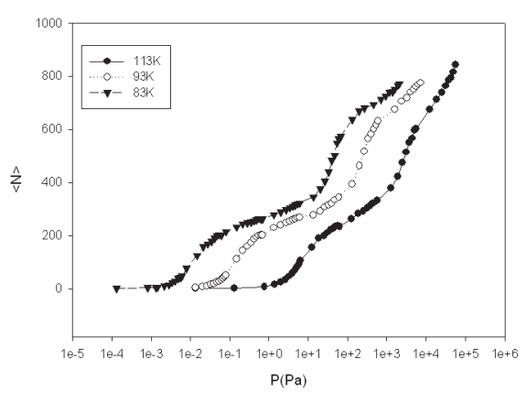

Fig. 11. Simulated isotherm at 83, 93, and 113 K for closed end tubes of diameter 1.628 nm (12,12) SWNT (Adapted from Albesa et al., 2010) Copyright 2010 American Chemical Society

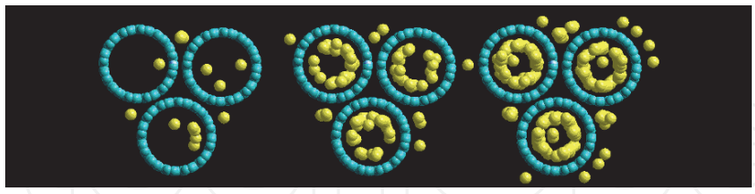

Fig. 12. Upper view of filling evolution corresponding to isotherm at 113 K and pressures of 1.38, 6.27, 56.3 Pa for opened end tubes of 1.628 nm, (12,12) SWNT. (Adapted from Albesa et al., 2010) Copyright 2010 American Chemical Society

4. Gas separation of nitrogen-oxygen and ethane-ethylene mixtures

Most commercial processes used in air separation employed synthetic zeolites. These materials are selective with respect to nitrogen, that is, they are able to adsorb more nitrogen than oxygen in a rate 4:1, due to the interaction between nitrogen molecule and oxygen cation to compensate charges. However find some kind of adsorbent that prefer oxygen is also interesting, because to reach the same separation than zeolites will only require a

quarter of work (Jayaraman & Yang, 2005). Among different substrates that have greater affinity with oxygen, carbonaceous materials are promising options (Arora & Sandler, 2007), being their principal use as selective sieves. Beside the isotherms, and the isosteric heat of adsorption, selectivity is other quantity of interest, selectivity of specie 1 respect to specie 2 is defined as:

$$S_{12} = (\theta_1/\theta_2)/(p_1/p_2) \tag{14}$$

where θ_i, and p_i, (i = 1, 2) are the relative coverage and partial pressure respectively, and, when there is no interaction between adsorbed species, it only depends on temperature , T, otherwise it is function of θ_1, θ_2 and T. In previous sections it was mention that adsorption explorations at molecular levels, i.e. by MCS, imply to select a model, and in case of gas mixtures, choose one approach enough simply to reduce computing time, but preserving the essential characteristics, becomes critical. One possibility is consider the molecules as pseudo spheres, that is only one Lennard – Jones interaction site per molecule (1CLJ), and a more realistic one would be consider molecules as composed by two interaction sites (2CLJ). We make a comparison of these two models for the adsorption of oxygen and nitrogen mix similar to the air composition, i.e. 80% and 20 % respectively. A remarkable difference appears in selectivity (Fig.13) because 1CLJ approximation gives fewer adsorption of nitrogen than oxygen, although the difference between adsorbed quantities is not high, reflects an important increase of the 1CLJ model selectivity. In Figure 14 we also note that the adsorption for 2CLJ model begins a lesser pressures than in the case of 1CLJ model. The density profiles (Figs. 15 and 16) show that the increase of pressure in 1CLJ model moves some molecules from the first layer to the second layer, so for nitrogen as for oxygen. In 2CLJ approximation this moving occurs basically with oxygen, while the density of the nitrogen first layer increase, this behavior, opposite to what one would hope from the entropic point of view according to the molecules size, is due to temperature considered, because greater temperatures favor nitrogen adsorption

Given that carbon nanotubes have internal sites that, after activation, are available for adsorption, and these have a narrow pore size distribution, these materials are presented as a promising alternative as adsorbents capable of achieving a good separation between N_2 and O_2.

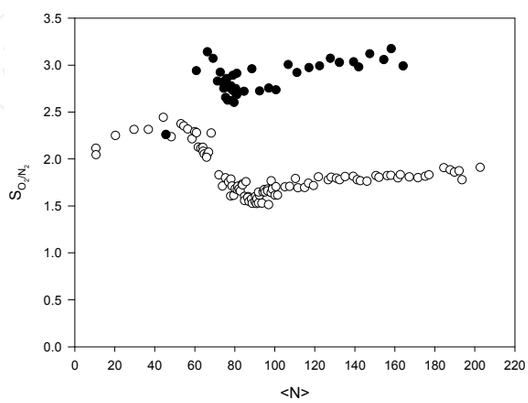

Fig. 13. Simulated selectivity at 100 K of air on graphite for 1CLJ (black) and 2CLJ (white) models. Total: squares, oxygen: triangles, and nitrogen: circles

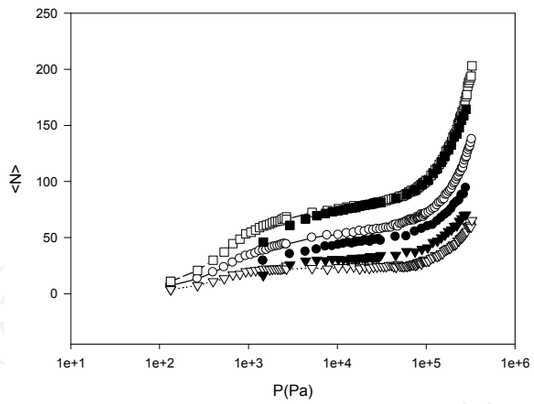

Fig. 14. Simulated adsorption isotherm at 100 K of air on graphite for 1CLJ (black) and 2CLJ (white) models. Total: squares, oxygen: triangles, and nitrogen: circles

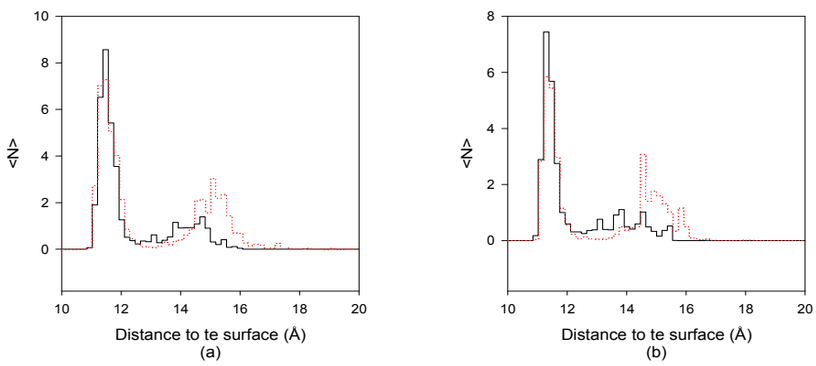

Fig. 15. Density profiles ρ as a function of the distance to the surface for 1CLJ model. Solid lines represent the results at 5866.1680 Pa and dotted lines at 45462 Pa (a)Nitrogen (b) Oxygen

By comparing the results obtained by Monte Carlo simulations in nanotubes (Fig. 17 a-c) with those obtained in graphite is observed that both materials show similar trends: there is a maximum degree of separation every time a monolayer is completed. As the nanotubes can complete an inner and outer monolayer, there are two peaks in the separation. Nanotubes with greater separation power are the *(10,10)*, diameter *1.356 nm*. As shown in the figures, the separation process takes place inside the nanotubes.
The degree of separation on the outer surface is negligible. From this arises the importance of obtaining good methods of activation, since the presence of interstitial defects (which are the size of the order of the nanotubes *(7,7)*, diameter *0.949 nm*) decreases significantly the separation of these mixtures.
Olefin – paraffin separation represents one of the most important separations in chemical and petrochemical industries. The production of plastics, rubbers, films, and other chemicals from olefins such as ethylene, requires high purity olefins (> 99%). Ethylene is generally produced by cracking or thermal decomposition of ethane, and during these processes the gas is an ethane and ethylene mix. The conventional cryogenic distillation is as efficient and reliable, and continues being the leading technology for ethane/ethylene separation; however, it is also energetic expensive due to the similar volatility of ethane and ethylene. In a typical ethylene plant, the cracking apparatus represent approximately 25% of the unit const, while the other 75% is due to compression, calefaction, dehydration, recovering and refrigeration systems (Anson et al., 2008).

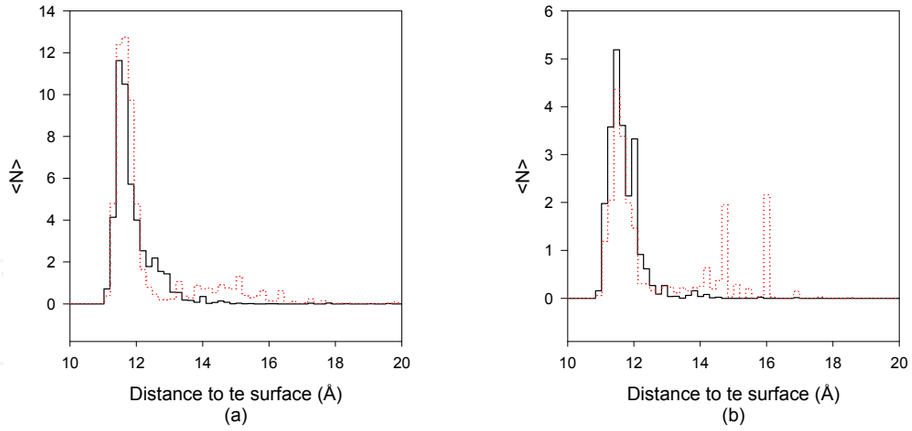

Fig. 16. Density profiles ρ as a function of the distance to the surface for 2CLJ model. Solid lines represent the results at 5866.1680 Pa and dotted lines at 45462 Pa(a)Nitrogen (b) Oxygen

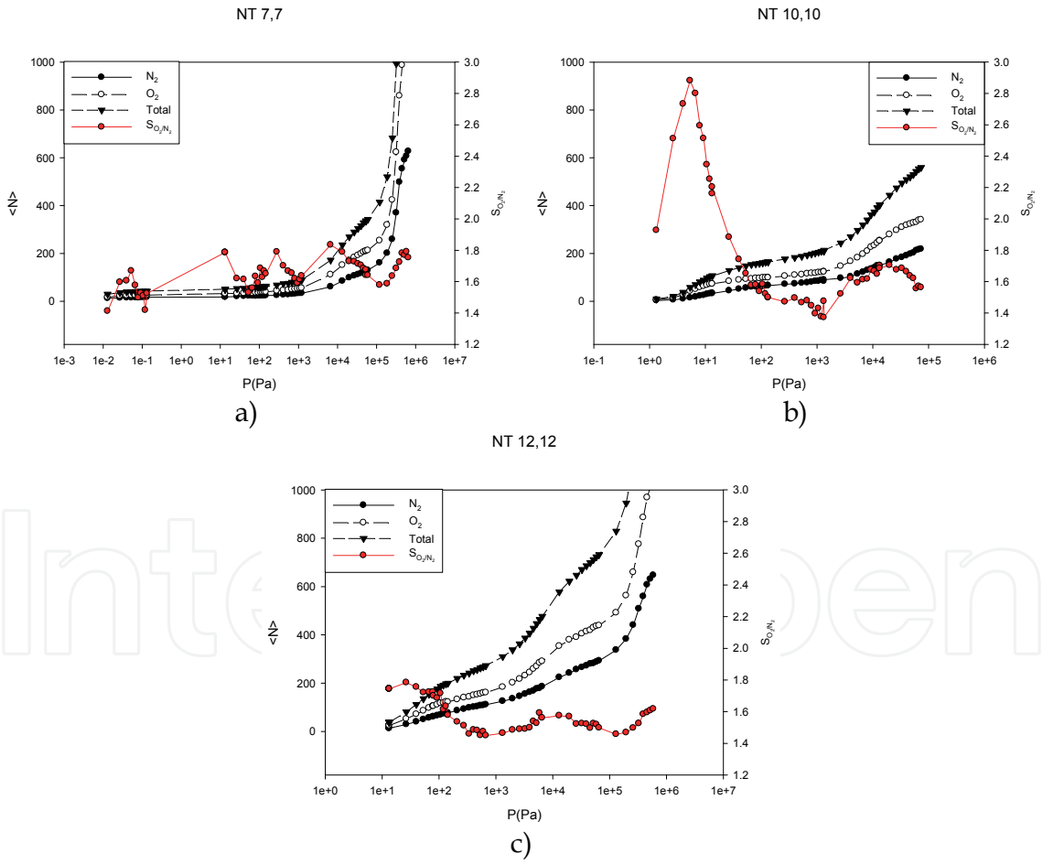

Fig. 17. Simulated isotherm 100 K and separation degree (right offset) for open nanotubes (a) (7,7) ; (b) (10,10); (c) (12,12)

An effective separation method that produces raw materials with highly ethylene enrichment without using cryodistillation would reduce the energetic and equipment costs

associated with paraffin/olefin separation. Therefore exist interest to develop new separation techniques (Fuentes & Mendez, 2002). Many alternative separations have been investigated, including chemical, extractive distillation, physical adsorption, and separation of the base membrane (Eldridge, 1993). Adsorption is one alternative to separation, which is till under develop. Adsorbent materials are generally incorporated joined to transition metals (copper or silver), and as a result the preferential adsorption of olefin is obtained. This selective adsorption is due to the strong interaction between non saturated olefins bonds and the metal ion on the surface, forming a π complex. Because of the preferential way in which olefin is adsorbed (Anson et al., 2010) by these substance it is possible to obtain paraffin pure. However, when paraffin selective adsorbed, olefin pure can be obtained, which becomes adsorption as efficient alternative. Unfortunately there are few materials able to reach this separation (Herdes et al., 2007). This preferential adsorption is due fundamentally to the interaction between methyl sites of the adsorbent and the adsorbat (Kroon & Vega, 2009).

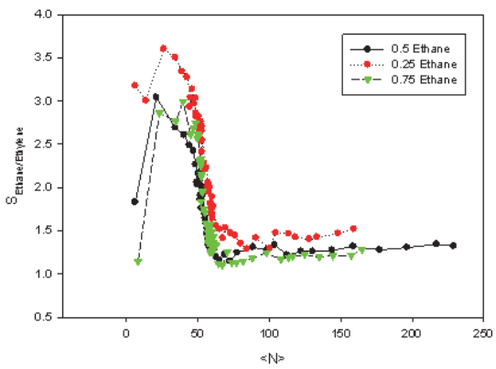

Fig. 18. Selectivity for ethane/ethylene in graphite as a function of the number of adsorbed molecules

It is well known that for only one component, the adsorption on carbonaceous materials is greater for ethane that ethylene. That is why these materials are studying when one is looking for a highly pure ethylene.
The simulation results show that the selectivity (Fig. 18), as a function of the number of adsorbed molecules, reaches a maximum when the monolayer is completed, as it happen with nitrogen – oxygen mixtures.
The profile is the same for all the compositions studied. The decrease in the degree of separation occurs because, once filled the monolayer, the adsorption of ethylene occurs more rapidly than ethane (Fig. 19 a-c). At high concentrations of ethylene, the number of molecules of ethane decreases, i.e., ethylene displaces ethane (Fig. 19 a). Here we see two phenomena, the principle of selective adsorption of ethane is due to energetic effects. As pressure increases the entropic effects are greater and that is why, because of their size, increases the adsorption of ethylene
Isosteric heat of adsorption of the mix is quite similar to the corresponding values of pure substances. It is also observed that there isn't a great variation of isosteric heat of adsorption with composition.(Fig 20 a-b)
A similar situation is observed in the adsorption of mixtures of nanotubes *(7,7)*; where the main adsorption takes place on the surface. Although in this case the coefficient of ethane-ethylene separation (Fig 21) is less than in the case of graphite.

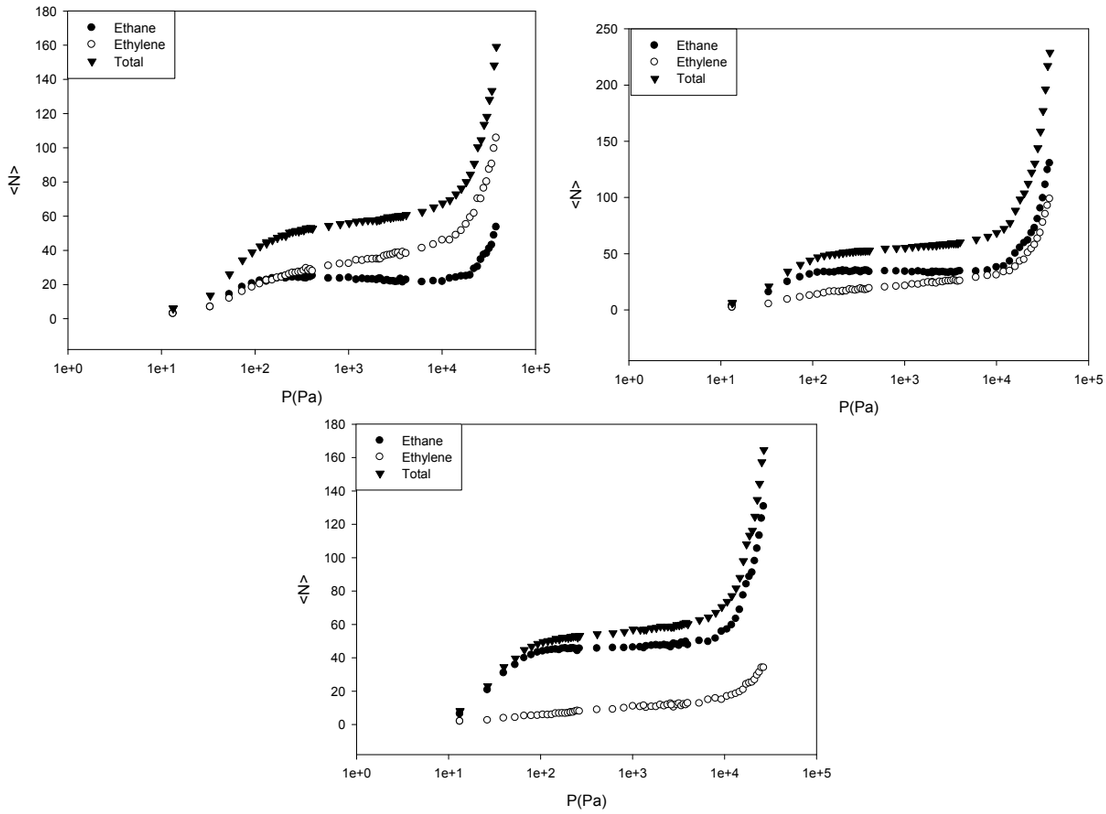

Fig. 19. Simulated adsorption isotherm at 153 K of ethane/ethylene mixtures on graphite for different compositions (a) 25%Ethane (b)50%Ethane (c)75%Ethane

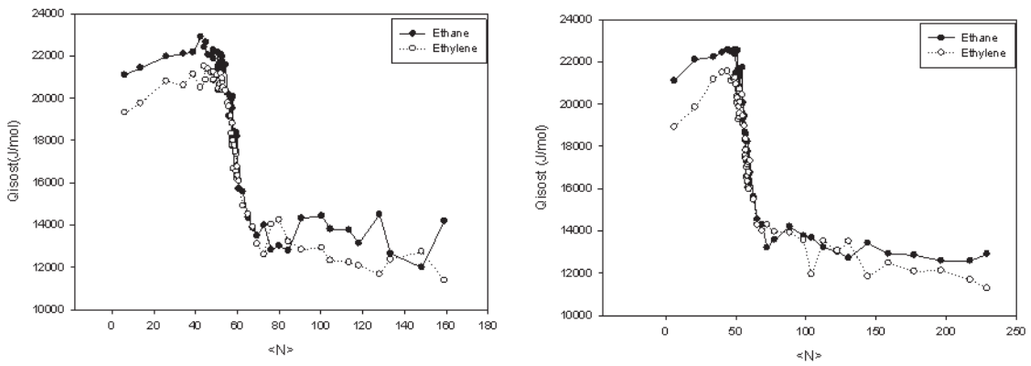

Fig. 20. Isosteric heat of adsorption at 153 K for ethane/ethylene mixtures on graphite for different compositions (a) 25%Ethane (b)75%Ethane

In this substrate the displacement of ethane molecules by ethylene which is observed in graphite is not present. The effect can be attributed to the curvature of this kind of nanotubes; this is, the small diameter provokes a less compact arrangement of the molecules, and therefore a less important effect of the entropic factors.

If we now consider nanotubes with larger diameters, so that adsorption occurs in the interior of them, we note that, as in the case of mixtures of nitrogen and oxygen, the

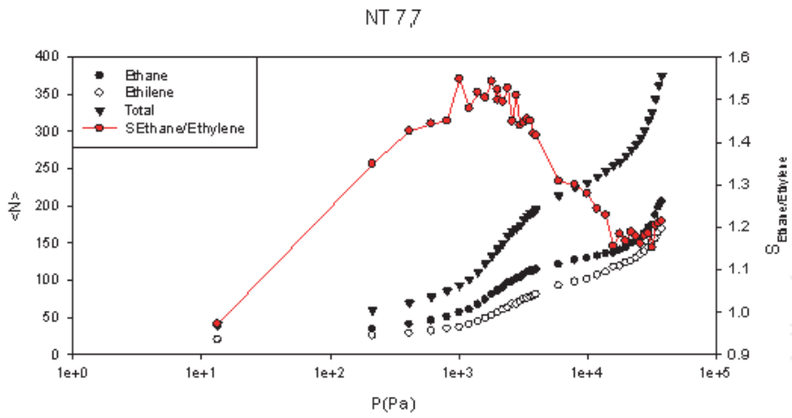

Fig. 21. Isotherms and Selectivity (right offset) for ethane/ethylene in *(7,7)* nanotubes as a function of the pressure

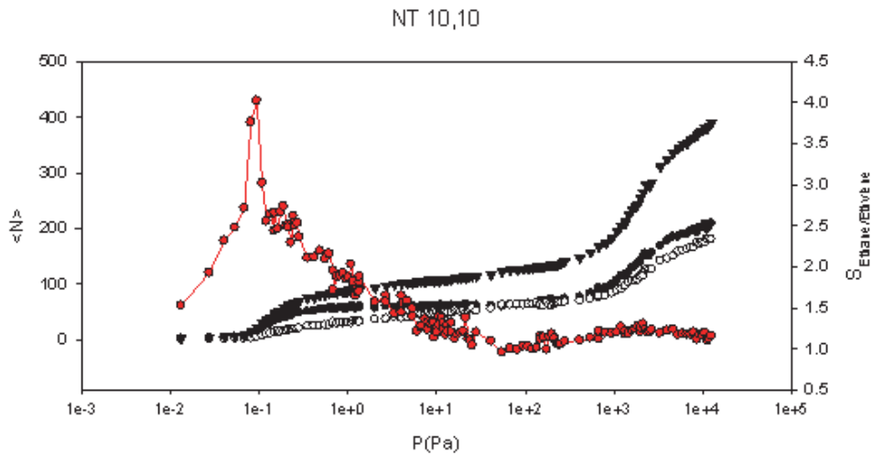

a)

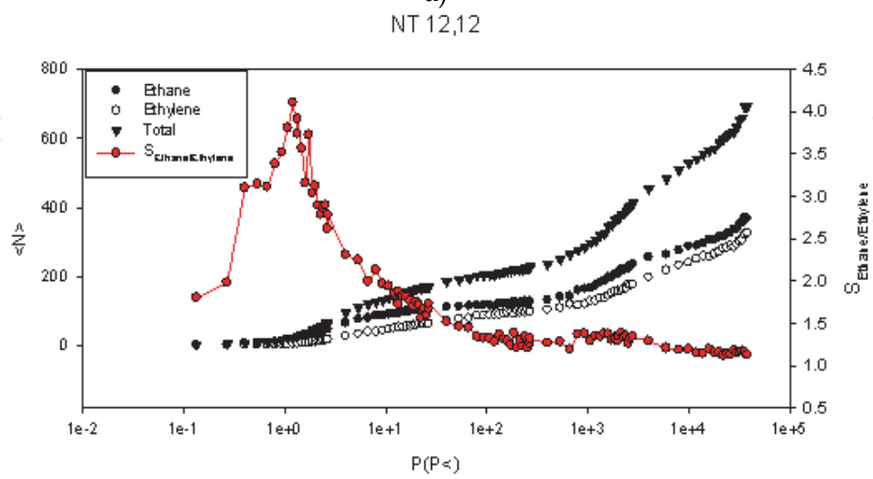

b)

Fig. 22. Isotherms and Selectivity (right offset) for ethane/ethylene as a function of the pressure in a) *(10,10)* nanotubes b) in *(12,12)* nanotubes

separation on the outside is very small, being slightly greater than one. Also note that the degree of separation in nanotubes *(10,10)* and the *(12,12)* (diameters *1.356 nm* and *1.628 nm* respectively) is practically the same (Figs. 22a and 22b). However, we can see that the positions of the maxima occur at different pressures. In this way, having a size distribution of nanotubes can enhance the range of pressures that are working.
Of particular interest is that the results obtained in systems nitrogen / oxygen and ethane / ethylene for the case of graphite, show similar trends to those obtained from more complex substrates, such as carbon nanotubes. This is why the above mentioned studies provide rich information on new systems, because, thanks to its structural simplicity, experiments can be carried out with great precision.

5. Conclusions

Experimental results of methane adsorption at low temperature, confirm a layer–by–layer filling mechanism, where the first two layers are clearly defined, but above 113 K this mechanism disappears and all layers are available to be filled. MCS confirm the necessity to employ atomist models in order to describe the adsorption a higher pressures, beyond that at very low pressures simple analytic models give good results with cheaper computational cost. The production of changes on the arrangement of adsorbed molecules as surface coverage increases is also corroborated, at microscopic level, by quantum mechanical descriptions. Although the heat of adsorption constituted an experimental and theoretical useful tool to explore thermodynamic aspects of the adsorption process, and from can be easily determined from the experimental side, theoretical descriptions have to be considered with some details. For instance if the models deal with isotherms associated to ideal monolayer, with molecules laying in a plane at a fix distance of the surface, heat of adsorptions values obtained are well defined, but by using other models, perhaps more realistic, when molecules are not arranged on a plane but around a mean distance of the surface, the number of molecules needed to have values with low dispersion is higher than the usual employed in MCS. The comparison, between experimental results and those obtained from MCS with different model approximations, confirms previous asseveration. In addition, Mean Field Approximation confirms that lower density values, similar to those derived from MCS by employing atomistic model, fit better experimental isotherms than the higher densities obtained from other models.
By considering curved graphene surfaces one can explore the adsorption on other types of graphitic structures (carbon nanotubes, nanocones, and others kinds of fullerenes). In spite DFT calculations of the interaction energy between the curved graphene substrates and simple molecules, reveals that surface potential energy is almost independent on the curvature, at least when these curvatures range values corresponding to common nanotubes; these kind of carbonaceous structures have many others adsorption sites that have to be explored. As an example, single walled nanotubes (SWNT) form bundles of various tubes, and then, besides the previous mentioned convex external wall sites (S), where the adsorption is a two dimensional process, other kinds of sites can appear. One are sites lying between two adjacent outer nanotubes of the bundle or groove sites (G), associated to one dimensional adsorption, other sites are similar to those founded in cylindrical pores, and emerge when tubes diameter are so higher that they left interstitial

channels (IC) with enough space in order to accommodate adsorbed molecules in them; and finally, and eventually they have inner sites (T) when there are SWNTs with their ends open. Beyond DFT calculations, where the energy of each sites confirm the postulated adsorption sequence: starts at the linear chains of G sites, and then in IC, if there are any one with enough space to accommodate molecules inside them, and finally on S sites. In case of open sites T sites have to be filled before G sites. MCS gives information about the shape of the isotherms, for instance, in case of open tubes, on the curve emerge a knee when a monolayer starts forming on the inside surface of the tubes, and also when this interior layer is completed.

By comparing these results with adsorption on graphite, one observes two facts: the monolayer of graphite is completed at a pressure below that corresponding to the nanotubes, and the isosteric heat of adsorption is greater for graphite, the reason is because the nanotubes considered are single walled (one graphene layer, rolled up) while graphite is formed by several graphene layers.

Results obtained from the study of gas mixtures adsorption (nitrogen / oxygen and ethane / ethylene) on different carbonaceous structures, show that graphite and more complex surfaces (such as carbon nanotubes) present similar trends. In this way, the behavior above described will provide valuable information on new systems.

6. Acknowledgment

The authors gratefully acknowledge financial support from the UNLP (Universidad Nacional de La Plata), CICPBA (Comisión de Investigaciones Científicas de la Provincia de Buenos Aires) and CONICET (Consejo de Investigaciones Científicas y Tecnológicas)

7. References

Albesa, A.G.; Llanos, J.L. & Vicente, J.L. (2008). Comparative study of methane adsorption on graphite. *Langmuir*, Vol. 24, pp. 3836-3840

Albesa, A.G. & Vicente, J.L. (2008). Theoretical study of methane adsorption on graphite. *The Journal of the Argentine Chemical Society*, Vol. 95, No. 1-2, pp. 10-22

Albesa, A.G.; Filippin, A. & Vicente, J.L. (2009). Effects of the Surface Curvature on the Adsorption of Simple Gases over Carbonaceous Materials using the Density Functional Theory (DFT) *CIT Technologic Information Review*, Vol. 29, pp. 31-37

Albesa, A.G.; Fertitta, E.A. & Vicente, J.L. (2010). Comparative Study of Methane Adsorption on Single-Walled Carbon Nanotubes. *Langmuir*, Vol. 26, pp. 786-795

Anson, A.; Wang, Y.; Lin, C.C.H.; Kuznicki, T.M. & Kuznicki, S.M. (2008). Adsorption of ethane and ethylene on modified ETS-10. *Chemical Engineering Science*, Vol. 63, pp. 4171-4175

Anson, A.; Lin, C.C.H.; Kuznicki, T.M. & Kuznicki, S.M. (2010). Separation of ethylene/ethane mixtures by adsorption on small-pored titanosilicate molecular sieves. *Chemical Engineering Science,* Vol. 65, pp. 807-811

Arora, G. & Sandler, S. (2007). Nanoporous carbon membranes for separation of nitrogen and oxygen: Insight from molecular simulations. *Fluid Phase Equilibria*, Vol. 259, pp. 3-8

Azami, T.; Kasuya, D.; Yuge, R.; Yudasaka, M.; Iijima, S.; Yoshitake, T. & Kubo, Y. (2008). Large-Scale Production of Single-Wall Carbon Nanohorns with High Purity. *J. Phys. Chem.,* Vol. 112, pp. 1330-1334

Bandosz, T.J.; Biggs, M.J.; Gubbins, K.E.; Hattori, Y.; Iiyima, T.; Kaneko, K.; Pikunic, J. & Thomson, K.T. (2003). Molecular Models of Porous Carbons, In: *Chemistry and Physics of Carbon,* Vol. 28, Marcel Dekker, Inc., L.R. Radovic, (Ed), pp. 41-228, ISBN 0-8247-0987-X, New York, USA

Baudu, M.; LeCloirec, P. & Martin, G. (1993), First approach of desorption energies of water and organic molecules onto activated carbon by differential scanning calorimetry studies. *Water Res.*, Vol. 27, pp. 69-76

Beaver, M. & Sircar, S. (2010), Methane Reforming Using a Novel Sorption Enhanced Reaction Concept, In: *Clean Energy Systems and Experiences*, InTech, K. Eguchi (Ed.), Viena, Austria

Bertoncini, C.; Odetti, H. & Bottani, E.J. (2000). Computer Simulation of Phenol Physisorption on Graphite. *Langmuir,* Vol. 16, pp. 7457-7463

Bhatia, S.K. & Myers, A.L. (2006). Optimal Conditions for Adsorptive Storage. *Langmuir*, Vol. 22, pp. 1688-1700

Bienfait, M.; Zeppenfield, P.; Dupont – Pavlovsky, N.; Muris, M.; Johnson, M.R.; DePie, M. & Vilches, O.E. (2004). Thermodynamics and structure of hydrogen, methane, argon, oxygen, and carbon dioxide adsorbed on single-wall carbon nanotube bundles. *Phys. Rev. B*, Vol. 70, pp. 035410

Bottani, E.J. & Bakaev, V.A. (1994), The Grand Canonical Ensemble Monte Carlo Simulation of Nitrogen on Graphite. *Langmuir*, Vol. 10, pp. 1550-1555

Burley, D.M. (1972) Col.2, pp. 329, In*: Phase Transitions and Critical Phenomena*; Academic Press, C. Domb & M.S. Green (Eds.), London, Great Britain

Cheng, A. & Steele, W.A. (1990). Computer Simulation Study of the Chemical Potential of Argon Adsorbed on Graphite. *Mol. Simulation*, Vol. 4, pp. 349-359

Cheng, H.; Cooper, A.C.; Pez, G.P.; Kostov, M.K.; Piotrowski, P. & Stuart, S.J. (2005), Molecular Dynamics Simulations on the Effects of Diameter and Chirality on Hydrogen Adsorption in Single Walled Carbon Nanotubes *J. Phys. B*, Vol. 109, pp. 3780-3786

De Oliveira, M.J. & Griffiths, R.S. (1978). Lattice-gas model of multiple layer adsorption. *Surf. Sci.*, Vol. 71, pp. 687-694

Do, D.D. & Do, H.D. (2005). Evaluation of 1-Site and 5-Site Models of Methane on Its Adsorption on Graphite and in Graphitic Slit Pores. *J. Phys. Chem. B*, Vol. 109, pp. 19288-19295

Dresselhaus, M.S.; Dresselhaus, G.D.; Eklund, P.C. (1996), *Science of Fullerenes and Carbon Nanotubes,* Academic Press (Ed.), New York, USA

Eldridge, A. (1993). Olefin/paraffin separation technology: a review. *Industrial & Engineering Chemistry Research,* Vol. 32, pp. 2208

Fuentes, A.B. & Mendez, I. (2002), Separation and Purification Technology, Vol. 28, pp. 29

Gravelle, P.C.J. (1978), Methods for the determination of heats of adsorption. *Therm. Anal.*, Vol. 14, pp 53-77

Groszek, A.J. (1998). Flow adsorption microcalorimetry *Thermochim. Acta*, Vol. 312, pp. 133-143

Hamilton, J.J. & Goodstein, D.L. (1983),.Thermodynamic study of methane multilayers adsorbed on graphite.*Phys. Rev. B*, Vol. 28, pp. 3838-3848

Harris, P.J.F. (2003). Impact of the Discovery of Fullerenes on Carbon Science, In: *Chemistry and Physics of Carbon,* Vol. 28, Marcel Dekker, Inc., L.R. Radovic, (Ed), pp. 1-40, ISBN 0-8247-0987-X, New York, USA

Herdes, C.; Valente, A.; Lin, Z.; Rocha, J.; Coutinho, J.A.P.; Medina, R.; Vega, L.F. (2007). Selective Adsorption of Volatile Organic Compounds in Micropore Aluminum Methylphosphonate-α: A Combined Molecular Simulation−Experimental Approach. *Langmuir*, Vol. 23, pp. 7299

Jayaraman, A. & Yang, R.T. (2005). Stable oxygen-selective sorbents for air separation . *Chemical Engineering Science*, Vol. 60, pp. 625-634

Kim, H.Y & Steele, W.A. (1992) Computer-simulation study of the phase diagram of the CH_4 monolayer on graphite: Corrugation effects. *Phys. Rev. B*, Vol. 45, pp. 6226-6233

Kostov, M.K.; Cheng, H.; Cooper, A.C. & Pez, G.P. (2002), Influence of Carbon Curvature on Molecular Adsorptions in Carbon-Based Materials: A Force Field Approach. *Phys. Rev. Lett.*, Vol. 89, pp 146105- (1-4)

Kroon, M.C. & Vega, L.F. (2009). Selective Paraffin Removal from Ethane/Ethylene Mixtures by Adsorption into Aluminum Methylphosphonate-α: A Molecular Simulation Study. *Langmuir*, Vol. 25, pp. 2148-2152

Krungleviciute, V; Calvi, M.M.; Wagner, J.A.; Migone, A.D.; Yudasaka, M. & Iijima, S. (2008). Probing the Structure of Carbon Nanohorn Aggregates by Adsorbing Gases of Different Sizes. *J. Phys. Chem*., Vol. 112, pp. 5742-5746

Krungleviciute, V; Migone, A.D. & Pepka, M. (2009). Characterization of single-walled carbon nanohorns using neon adsorption isotherms. *Carbon*, Vol. 47, pp. 769-774

Kuznetsova, A.; Yates, J.; Liu, J. & Smalley, R.E. (2000) *J. Chem. Phys. 112*, 9590−9598

Llanos, J.L.; Fertita, A.E.; Flores, E.S. & Bottani, E.J. (2003), SO_2 Physisorption on Exfoliated Graphite**.** *J. Phys. B*, Vol. 107, pp. 8448-8453

Myers, A.L. & Prausnitz, J.M. (1965), Thermodynamics of mixed-gas adsorption.AIChE, J., Vol. 11, pp. 121-127

Nicholson, D. & Parosonage, N.G. (1982), *Computer Simulation and the Statistical Mechanics of Adsorption*, Academic Press (Ed.), London, Great Britain

Niyogi, S.; Hamon, M.A. ; Hu, H. ; Zhao, B. & Bownik, S. (2002), Chemistry of Single-Walled Carbon Nanotubes. *Acc. Chem. Res*., Vol. 35, pp. 1105-1113

Okamoto, Y. & Miyamoto, Y. (2001), Ab Initio Investigation of Physisorption of Molecular Hydrogen on Planar and Curved Graphenes.*J. Phys. Chem. B*, Vol. 105 (17), pp. 3470-3474

Parr, R.G. & Perdew, J.P. (1989), *Density Functional Theory of Atoms and Molecules,* Oxford University Press (Ed.), Oxford, Great Britain

Pascual, P.; Ungerer, P.; Taviatan, B.; Pernot, P. & Boutin, A. (2003). Development of a transferable guest–host force field for adsorption of hydrocarbons in zeolites I. Reinvestigation of alkane adsorption in silicalite by grand canonical Monte Carlo simulation. *Phys. Chem. Chem. Phys*., Vol. 5, pp. 3684-3693

Piper, J. & Morrison, J.A. (1984). Heats of adsorption of methane multilayers on graphite *Phys. Rev. B*, Vol. 30, pp. 3486-3489

Sabzyan, H. & Babajani, M. (2005), A semiempirical quantum mechanical study of methane–graphite interaction. *J. Molec. Struct. : THEOCHEM,* Vol. 726, pp. 155-160

Scheele, C.W. (1777). *Chemische Abhandlung fon der Luft un dem Feuer,* Akad.d.Wiessenschaft Mitgliedes, Leipzig, Germany

Steele, W.A. (1973). The physical interaction of gases with crystalline solids: I. Gas-solid energies and properties of isolated adsorbed atoms. *Surf. Sci*., Vol. 36, pp. 317-352

Steele, W.A. (1974), *The interaction of Gases with Solid Surfaces*, Pergamon Press (Ed.), ISBN 10-0080-177247, Oxford, Great Britain

Talapatra, S. & Migone, A.D. (2002). Adsorption of methane on bundles of closed-ended single-wall carbon nanotubes**.** *Phys. Rev. B,* Vol. 65, pp. 045416(1-6)

Tasca, R.A.; Calbi, M.M. & Cole, M.W. (2002), Lattice model of gas condensation within nanopores. *Phys. Rev. E*, Vol. 65, pp. 061607(1-9)

Vilaplana, A.F. (2005) Ab initio computational investigation of physisorption of molecular hydrogen on achiral single – walled carbon nanotubes, *J. Chem. Phys*.: 122, 214724-1-7

Wagner, K. (1996). Methane, In: *International thermodynamics tables of the fluids state,* Vol. 13, IUPAC chemical data series, Blacwell Sciece (Ed.), Boston, USA

Wang, Y. & Perdew, J.P. (1991), Correlation hole of the spin-polarized electron gas, with exact small-wave-vector y high-density scaling, *Phys. Rev B*: 44(24), 13298-13307

Wang, Y. & Johnson, J. (1999). Molecular simulation of hydrogen adsorption in single-walled carbon nanotubes y idealized carbon slit pores, *J. Chem. Phys.:* 110 577-586

Wuebbles, D.J. & Hyhoe K. (2000), Atmospheric Methane: Trends and Impacts, In: *Non CO_2 greenhouse gases,* Springer Verlag, J. van Ham (Ed.), Amsterdam, Holland

Yudasaka, M.: Iijima, S. & Crespi, V.H. (2008), Single Wall Carbon Nanohorns and Nanocones, In: *Carbon Nanotubes, Topics Appl. Physics,* 111, 605, Springer Verlag, A. Jorio; G.D. Dresselhaus & M.S. Dresselhaus (Eds.), Berlin, Germany

Zettlemoyer, A.C. & Narayan, K.S. (1966), *Chem. Phys. Carbon*, Vol. 2, pp. 197

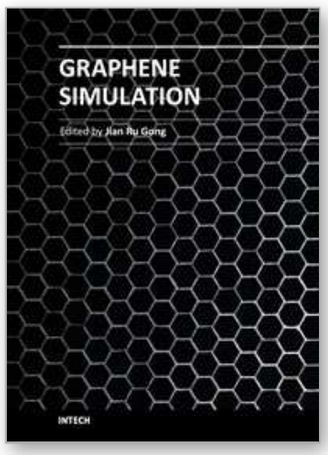

Graphene Simulation
Edited by Prof. Jian Gong

ISBN 978-953-307-556-3
Hard cover, 376 pages
Publisher InTech
Published online 01, August, 2011
Published in print edition August, 2011

Graphene, a conceptually new class of materials in condensed-matter physics, has been the interest of many theoretical studies due to the extraordinary thermal, mechanical and electrical properties for a long time. This book is a collection of the recent theoretical work on graphene from many experts, and will help readers to have a thorough and deep understanding in this fast developing field.

How to reference
In order to correctly reference this scholarly work, feel free to copy and paste the following:

José L. Vicente and Alberto G. Albesa (2011). Description of Adsorbed Phases on Carbon Surfaces: A Comparative Study of Several Graphene Models, Graphene Simulation, Prof. Jian Gong (Ed.), ISBN: 978-953-307-556-3, InTech, Available from: http://www.intechopen.com/books/graphene-simulation/description-of-adsorbed-phases-on-carbon-surfaces-a-comparative-study-of-several-graphene-models

INTECH
open science | open minds

InTech Europe
University Campus STeP Ri
Slavka Krautzeka 83/A
51000 Rijeka, Croatia
Phone: +385 (51) 770 447
Fax: +385 (51) 686 166
www.intechopen.com

InTech China
Unit 405, Office Block, Hotel Equatorial Shanghai
No.65, Yan An Road (West), Shanghai, 200040, China
中国上海市延安西路65号上海国际贵都大饭店办公楼405单元
Phone: +86-21-62489820
Fax: +86-21-62489821

IntechOpen